Surface Plasmon Photodetectors Based on Noble Metals

© S. Benghorieb[1], A. Bouhadiche[1], S. Benzeghda[2], T. Touam[3,¶]

[1] Research Unit in Optics and Photonics (UROP),
Center for Development of Advanced Technologies (CDTA), University of Setif 1,
Setif, 19000 Algeria
[2] Microsystems and Instrumentation Laboratory, Department of Electronics, University Mentouri Constantine,
Constantine 25000, Algeria
[3] Semiconductors Laboratory, University Badji Mokhtar-Annaba,
Annaba 23000, Algeria

¶ E-mail: touamt@gmail.com

Received April 28, 2021
Revised October 10, 2021
Accepted for publication May 16, 2022

In this work, high sensitivity noble metals used in the Kretschmann configuration based photodetectors applied to detect the presence of biological and chemical species in solutions are investigated. The angle of incidence and film thickness dependencies of the surface plasmon polariton resonance (SPPR) of gold, silver and copper by the attenuated total reflection (ATR) method are studied to monitor and evaluate the SPR reflectance angle and reflectivity change. The analysis of the electric field of the surface plasmon wave which appears at the interface between the metallic layer and the air is carried out by the finite element method (FEM). The simulation is performed using COMSOL Multiphysics software which supports FEM. The aim of the present study is to find the most suitable noble metal and its optimum thickness to improve the performance of the SPR photodetector.

Keywords: Attenuated total reflection method, FEM based COMSOL multiphysics software, Kretschmann configuration, noble metals, reflectivity.

DOI: 10.21883/SC.2022.08.54121.9676a

1. Introduction

Plasmonic materials, when properly illuminated with visible or near infrared wavelengths, exhibit unique and interesting characteristics that can be exploited to tailor and adjust the radiation and propagation properties of light to nanoscale dimensions [1–8]. Various plasmonic structures have been exploited for optical signal filtering [9,10], switches [11,12], transport [13,14], modulation [15,16] and detection [17,18].

Surface plasmon resonance (SPR) devices have a high data rate of optical signals in photonic components and very small electronic circuit sizes can be developed through the synergistic integration of photonic, plasmonic and electronic components on the same chip [19].

Recent years have witnessed considerable progress in the exploitation of plasmonic nanostructures for the early diagnosis of several diseases [20,21]. Various biomarkers have been discovered and used by measuring concentrations in bodily fluids such as blood and saliva [22–28].

Among the various analytical methods, the surface plasmon resonance biosensor is emerging as a potential detection platform due to its high sensitivity, selectivity and intuitive functionality [29–32]. The optoelectronic phenomenon of SPR, widely used in optical biosensors, is a resonant mode resulting from the coupling of electromagnetic waves and collective oscillations of free electrons on metal surfaces, especially noble metals among various biological photodetectors with high performance SPR biosensor based on a Kretschmann configuration [33–37]. It consists of a thin metal layer sandwiched between two dielectric media: a substrate and a biological medium to be studied. The metal film has multiple functions: as a grating coupler for *p*-polarized incident light and surface plasmons supported by the interface and exploiting the refractive effect in biological medium with the high sensitivity of strongly confined surface plasmons to the surrounding index.

This investigation concerns the modeling and simulation of the optical response of an SPR photodetector based on the Kretschmann configuration using noble metals: Au, Ag and Cu. The effect of various geometric parameters of the metal layer and the surrounding environment, and their impact on the optimization of the sensitivity and the precision of the sensors are studied. The profile of the electric field around structures, 2D modeling and simulation of SPR-based devices are studied using COMSOL Multiphysics software.

2. Simulation procedure: excited surface plasmon polaritons in the Kretschmann modell

Kretschmann's method uses a detection microscope that moves to different positions to give different angles as shown in Fig. 1. When the incoming light moves from the medium which has a higher refractive index to the medium with a lower refractive index, and the light impacts the interface between the two mediums at an angle greater than the critical angle, the light will be totally reflected. This

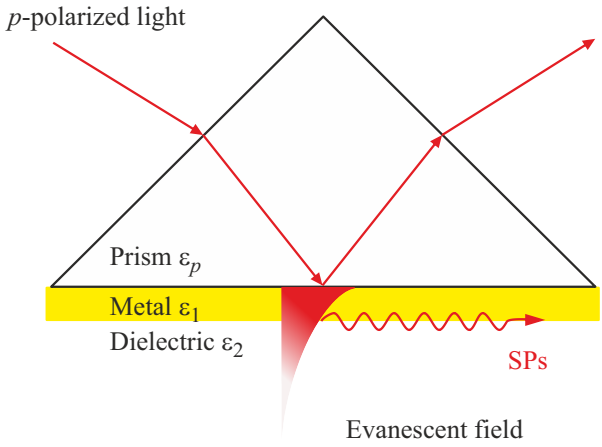

Figure 1. A schematic representation of Kretschmann configuration.

phenomenon is called Total Internal Reflection (TIR) [38]. TIR creates a kind of electromagnetic wave between the contact surfaces of the two media called an evanescent electromagnetic field [39]. The minimum amount of total internal reflection is observed when the incoming energy of the incident light is coupled to the flat metal. This is referred to „Attenuated Total Reflection" (ATR).

TM polarized incident light impacts the prism and activates the excitation of surface plasmon waves at the interface between the metallic thin film and the dielectric (air) layer. The wave vector of the light can be adjusted to be equal to the wave vector of the surface plasmon by launching it from the prism through the metallic thin film. The prism is a medium with a higher refractive index than the metallic film. Light traveling through the prism is reflected at the prism-metal layer interface by means of total internal reflection. The evanescent field of light reflected at the metal prism interface penetrates the metal [40]. With the appropriate thickness of the metal layer, the evanescent wave reaches the metal-dielectric interface (or metal-air interface). In the case that the phase of the incoming light propagating in the prism matches the phase of the surface plasmon waves, the surface plasmon resonance is generated and the surface plasmon waves propagate along this metal-dielectric interface. They are generated under a certain condition which depends on the angle of incidence and the wavelength.

The angular shift $\Delta\theta$ is the signature for the SPR detection of the biological medium. The biosensing Instrument's sensibility SR_θ is one of the most important parameters that determine its performance and is defined as follows

$$SR_\theta = \frac{\Delta\theta}{\Delta n}. \qquad (1)$$

3. Results and discussion

We study the interaction of SPR with material of different thicknesses in order to detect its effect on the evolution of resistance values and to choose the optimal thickness of the noble metal. Plasmon resonance reflection spectra are calculated using experimentally determined massive dielectric constants [41].

3.1. Interaction with matter

To investigate the properties of the SPR biosensor, we consider a thin metal layer with a thickness of 50 nm deposited on a SiO_2 prism and taking water as the dielectric medium. The system is excited with a light source at 633 nm.

The sensing characteristics of the devices are examined using two different materials: water and blood, with refractive indices of $n_{\text{water}} = 1.33$ and $n_{\text{blood}} = 1.38$, respectively. The reflectivity spectra of the model sensor are shown in Fig. 2; the angle of incidence is gradually changed by 1° from 40 to 80°. The results display two theoretical reflectance responses of a thin silver film 50 nm thick. The resonance angle of the Ag sensor shifts to a higher value as the refractive index of the surrounding medium increases; θ_R is 65.5° for pure water and 71.88° for blood. From Eq. (1), we obtain a sensitivity equals to 127°/RIU.

The performance of the sensor can be further extended by optimized geometric parameters of the photodetector. To assess the effect of the metallic film on the sensitivity of our sensor and determine the optimal metal for this device, four metals are selected in this study: Au, Ag, Cu and Al, with complex refractive indices of $0.1856 + i3.4201$, $0.056206 + i4.2776$, $0.26965 + i3.4106$ and $1.4495 + i7.5387$, respectively. The obtained results are depicted in Fig. 3

The detector will detect a reflectivity almost equal to 1, just when the excitation condition SP is met. For a particular angle and wavelength and when the coupling condition is satisfied, the light is very efficiently converted to SP. The reflectance drops off sharply, indicating SP excitation.

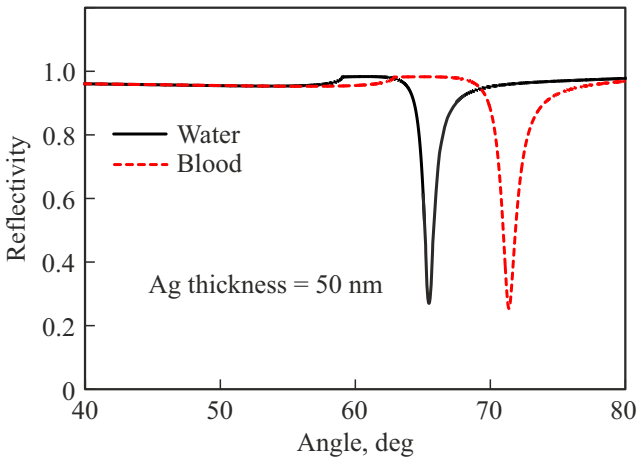

Figure 2. Reflection spectra of a 50 nm thick Ag film in two different surrounding media: water and blood.

When its value is close to 0, the confinement reaches its maximum and increases the accuracy of the sensor. The numerical results show that the noble metals have the ability to increase the sensitivity of the sensor [42] compared to the non-noble metals (Al); it is evident that a minimum value of reflectance R_{min} is observed for the Au film. In the reaction system, the Au film exhibits stability, strong adhesion with glass and does not produce any reaction with inorganic ions. In addition, Au is not susceptible to oxidation and generally does not react with most chemicals. On the other hand, copper and silver are great alternatives to gold.

The same study is carried out for a sensitive medium. Fig. 4 represents the variation of the photo-response as a function of the refractive index for three media: water, glycerol ($n_{glycerol} = 1.357$) and blood. By comparing the reflectance profiles, the lowest level of reflectivity R_{min} is observed as the refractive index of the surrounding medium decreases. The angular sensitivity of the Au sensor is 131.85°/RIU.

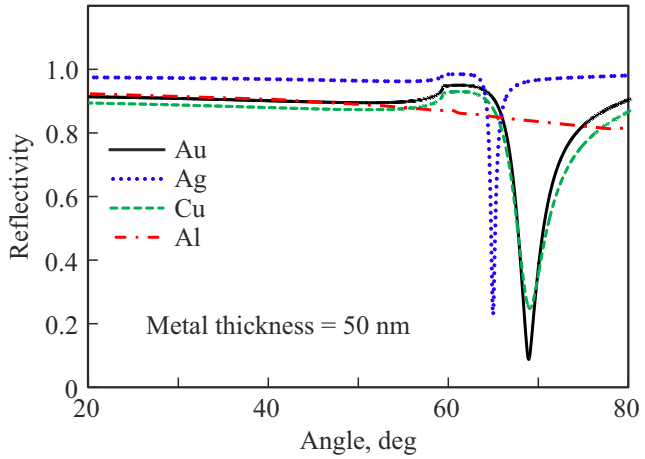

Figure 3. Reflection spectra of 50 nm thick Au, Ag, Cu and Al films in water.

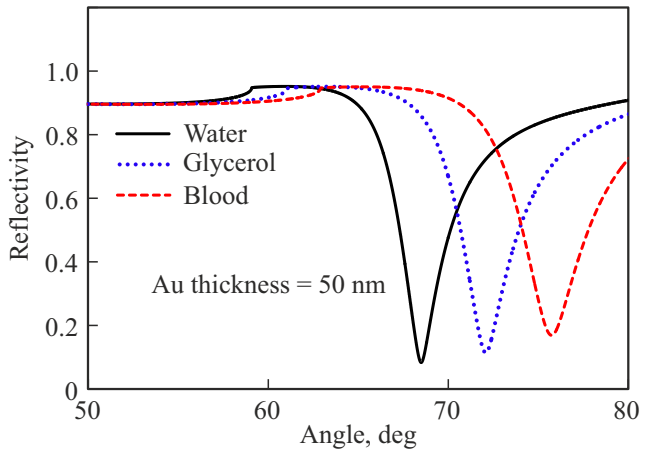

Figure 4. Reflection spectra of a 50 nm thick Au film in: water ($n_{water} = 1.33$), glycerol ($n_{glycerol} = 1.357$) and blood ($n_{blood} = 1.38$).

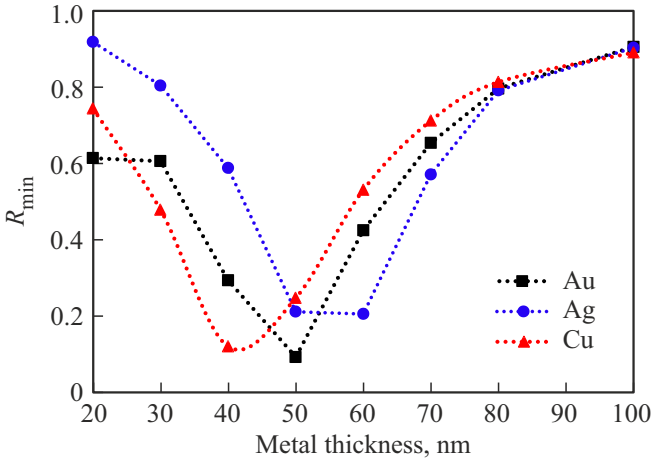

Figure 5. R_{min} of Au, Ag and Cu films in water as a function of the thickness of the metal.

In order to determine the optimum thickness of the metal film, the value of this input parameter is increased from 20 nm to 100 nm; the largest minimum reflectivity is clearly presented as a function of the thickness of the noble metals in Fig. 5.

The optimum thickness of the Au, Ag and Cu layers is approximately 50, 60 and 40 nm, respectively. As expected, the Au layer results in a smaller reflectivity; i. e. higher coupling efficiency compared to Ag and Cu: $R_{min\,Au} = 0.088$, $R_{min\,Ag} = 0.200$, $R_{min\,Cu} = 0.105$.

For the HeNe laser source, approximately 91, 89 and 80% of the incident light is reflected for the noble metals: Au, Cu and Ag, respectively, indicating an increase in the confinement of the plasmon at the metal-dielectric interface and an optimal SPR signature found for noble metals.

3.2. SPR field profile

The near-field behavior at the dielectric–metal–oxide interface is analyzed using COMSOL Multiphysics software based on the finite element method, where light (at 633 nm) from a HeNe laser propagates through a SiO_2 prism. In this case, a 50 nm thick Ag layer and a dielectric medium (water) are used. The thickness of the surrounding medium is greater than that of the metal; there are surface plasmon waves when the angle of incidence is 43.58°.

In the COMSOL wave optical RF module, the incident field is set at an input port to the limit indicated by specifying the z component of the magnetic field (TM-wave), while the reflected beam will be monitored at the port of exit.

The Floquet periodic boundary condition (FPBC) is imposed on all the lateral boundaries of the structure to satisfy the „semi-infinite“ condition of excitation of the SPs. To excite the SPs, it is necessary that the components of the electric field act along the metal-dielectric interface. Therefore, the SPs are only excited by the incident p-polarized

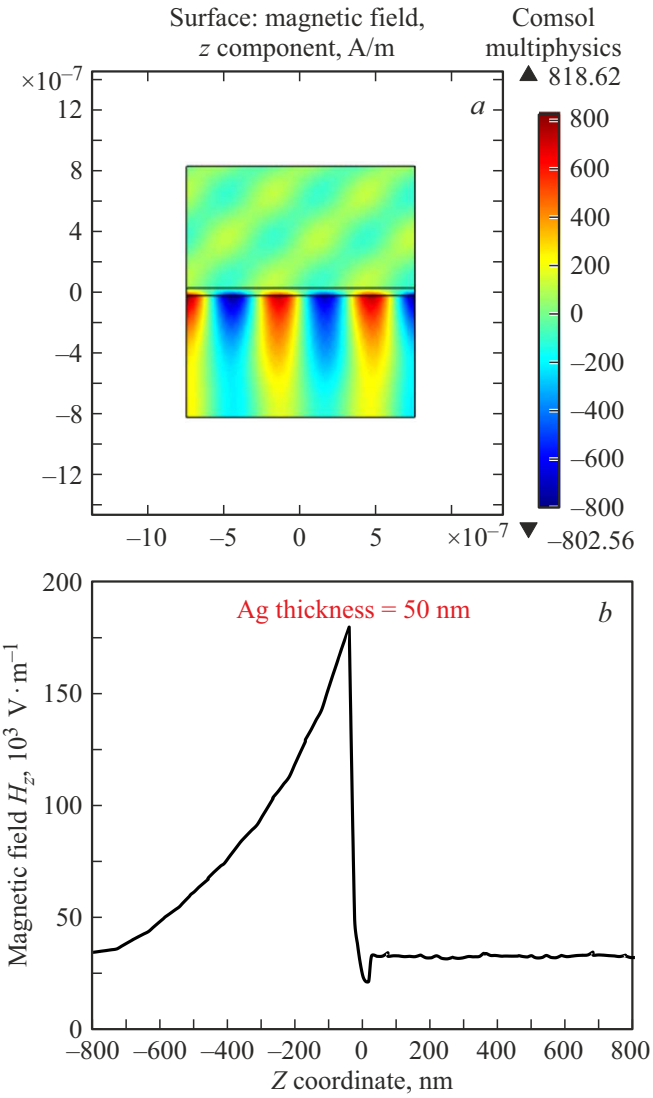

Figure 6. (*a*) 2D simulated field distribution at the resonance condition and (*b*) H_z magnetic field profile of a 50 nm thick Ag film in air.

light. *P*-polarized incident light refers to a transverse magnetic wave (H_{TM}) at port 1.

The characteristics of the electric field of the surface plasmon wave are different when the refractive index of the three layers is changed. The spatial extension of the electric field associated with the resonant wavelength for the model is shown in Fig. 6. Thanks to the SPR phenomenon, an exponential decrease in the electric field is observed on either side of the metal-dielectric; the variation of the intensity of the magnetic field H_Z over a cut line along the *z* axis.

4. Conclusions

Surface plasmon polariton (SPP) resonance spectra for noble metals (Au, Ag and Cu) have been extensively investigated in Kretschmann's Attenuated Total Reflection (ATR) geometry with an angle of incidence (θ) ranging from 20 to 80° and a film thickness (d) varies from 20 to 100 nm using different sensing media (pure water, glycerol and blood). The surface plasmon resonance angle, appearing as a dip in the reflection spectra, showed reasonable agreement with previously reported results. Our simulations demonstrated that film thickness significantly affected reflectivity. Optimal plasmon excitation in ATR geometry, where reflectivity became zero, was satisfied for the 40–60 nm thickness range of metal films. In terms of sensitivity, the surface plasmon resonance SPR produced high detection, amplifying the level of accuracy of the sensor. Comparing the three noble metals, Au was the ideal choice for detection. Copper, which is an economical noble metal, gives better conductivity than gold and theoretically has an optical response very close to that of gold; but it is more reactive, it is sensitive to the reaction with the detection medium.

Conflict of interest

The authors declare that they have no conflict of interest.

References

[1] S. Kasani, K. Curtin, N. Wu, Nanophotonics **8**, *12*, 2065 (2019).
[2] S.V. Boriskina, H. Ghasemi, G. Chen, Mater. Today **16**, *10*, 375 (2013).
[3] W.O.F. Carvalho, J.R. Mejía-Salazar, Sensors **20**, *9*, 2488 (2020).
[4] T. Umakoshi, M. Tanaka, Y. Saito, P. Verma, Sci. Adv. **6**, *23*, eaba4179 (2020).
[5] G.V. Naik, J.L. Schroeder, X. Ni, A.V. Kildishev, T.D. Sands, A. Boltasseva, Opt. Mater. Express **2**, *4*, 478 (2012).
[6] V.G. Kravets, A.V. Kabashin, W.L. Barnes, A.N. Grigorenko, Chem. Rev. **118**, *12*, 5912 (2018).
[7] H. Yu, Y. Peng, Y. Yang, Z.-Y. Li, npj Comput. Mater. **5**, *1*, 45 (2019).
[8] P. Khan, G. Brennan, J. Lillis, S.A.M. Tofail, N. Liu, C. Silien, Symmetry **12**, *8*, 1365 (2020).
[9] H.-J. Li, L.-L. Wang, J.-Q. Liu, Z.-R. Huang, B. Sun, X. Zhai, Appl. Phys. Lett. **103**, *21*, 211104 (2013).
[10] H.-J. Li, L.-L. Wang, B. Sun, Z.-R. Huang, X. Zhai, J. Appl. Phys. **116**, *22*, 224505 (2014).
[11] S. Khani, M. Danaie, P. Rezaei, Plasmonics **15**, 869 (2020).
[12] H. Mbarak, R.T. Ghahrizjani, S.M. Hamidi, E. Mohajerani, Y. Zaatar, Sci. Rep. **10**, *1*, 5110 (2020).
[14] J. Ghosh, G. Natu, P.K. Giri, Org. Electron. **71**, 175 (2019).
[14] J.E. Muench, A. Ruocco, M.A. Giambra, V. Miseikis, D. Zhang, J. Wang, H.F.Y. Watson, G.C. Park, S. Akhavan, V. Sorianello, M. Midrio, A. Tomadin, C. Coletti, M. Romagnoli, A.C. Ferrari, I. Goykhman, Nano Lett. **19**, *11*, 7632 (2019).
[15] C. Hoessbacher, A. Josten, B. Baeuerle, Y. Fedoryshyn, H. Hettrich, Y. Salamin, W. Heni, C. Haffner, C. Kaiser, R. Schmid, D.L. Elder, D. Hillerkuss, M. Möller, L.R. Dalton, J. Leuthold, Opt. Express **25**, *3*, 1762 (2017).

[16] Y. Salamin, P. Ma, B. Baeuerle, A. Emboras, Y. Fedoryshyn, W. Heni, B. Cheng, A. Josten, J. Leuthold, ACS Photonics **5**, *8*, 3291 (2018).
[17] C. Pacholski, S. Rosencrantz, R.R. Rosencrantz, R.F. Balderas-Valadez, Anal. Bioanal. Chem. **412**, *14*, 3433 (2020).
[18] J.C. Tong, F. Suo, J.H.Z. Ma, L.Y.M. Tobing, L. Qian, D.H. Zhang, Opto-Electron. Adv. **2**, *1*, 180026 (2019).
[19] J.-G. Walter, A. Eilers, L.S.M. Alwis, B.W. Roth, K. Bremer, Sensors **20**, *10*, 2889 (2020).
[20] G.A. Lopez, M.-C. Estevez, M. Solera, L.M. Lechuga, Nanophotonics **6**, *1*, 123 (2017).
[21] A. Genç, J. Patarroyo, J. Sancho-Parramon, N.G. Bastús, V. Puntes, J. Arbiol, Nanophotonics **6**, *1*, 193 (2017).
[22] B. Senf, W.-H. Yeo, J.-H. Kim, Biosensors **10**, *9*, 127 (2020).
[23] S. Williamson, C. Munro, R. Pickler, M.J. Grap, R.K. Elswick, Comparison of biomarkers in blood and saliva in healthy adults, Nurs. Res. Pract. **2012**, 246178 (2012).
[24] D.S.-Q. Koh G.C.-H. Koh, Occup. Environ. Med. **64**, *3*, 202 (2007).
[25] S. Hu, J.A. Loo, D.T. Wong, Proteomics **6**, *3*, 6326 (2006).
[26] L. Zhang, H. Xiao, D.T. Wong, Mol. Diag. Ther. **13**, *4*, 245 (2009).
[27] H. Jasim, A. Carlsson, B. Hedenberg-Magnusson, B. Ghafouri, M. Ernberg, Sci. Rep. **8**, *1*, 3220 (2018).
[28] L.A.S. Nunes, S. Mussavira, O.S. Bindhu, Biochem. Med. **25**, *2*, 177 (2015).
[29] J.-H. Choi, J.-H. Lee, J. Son, J.-W. Choi, Sensors **20**, *4*, 1003 (2020).
[30] J. Liu, M. Jalali, S. Mahshid, S. Wachsmann-Hogiu, Analyst **145**, *1*, 364 (2020).
[31] G. Zanchetta, R. Lanfranco, F. Giavazzi, T. Bellini, M. Buscaglia, Nanophotonics **6**, *4*, 627 (2017).
[32] W. Gong, S. Jiang, Z. Li, C. Li, J. Xu, J. Pan, Y. Huo, B. Man, A. Liu, C. Zhang, Opt. Express **27**, *3*, 3483 (2019).
[33] I. Abdulhalim, Nanophotonics **7**, *12*, 1891 (2018).
[34] S. Sharma, R. Kumari, S.K. Varshney, B. Lahiri, Rev. Phys. **5**, 100044 (2020),.
[35] G.S. Mei, P.S. Menon, G. Hegde, Mater. Res. Express **7**, *1*, 012003 (2020).
[36] A. Abbas, M.J. Linman, Q. Cheng, Biosens. Bioelectron. **26**, *5*, 1815 (2011).
[37] B.A. Prabowo, A. Purwidyantri, K.-C. Liu, Biosensors **8**, *3*, 80 (2018).
[38] K.J. Willis, J. Schneider, S.C. Hagness, Opt. Express **16**, *3*, 1903 (2008).
[39] N.L. Thompson, X. Wang, P. Navaratnarajah, J. Struct. Biol. **168**, *1*, 95 (2009).
[40] S. Ekgasit, C. Thammacharoen, W. Knoll, Anal. Chem. **76**, *3*, 561 (2004).
[41] P.B. Johnson, R.W. Christy, Phys. Rev. B **6**, *12*, 4370 (1972).
[42] M.G. Manera, A. Colombelli, A. Taurino, A.G. Martin, R. Rella, Sci. Rep. **8**, *1*, 12640 (2018).